

Reconstruction and interpretation of giant mafic dyke swarms: a case study of 1.78 Ga magmatism in the North China craton

PENG PENG

State Key Laboratory of Lithospheric Evolution, Institute of Geology and Geophysics, Chinese Academy of Sciences, Beijing 100029, China (e-mail: pengpengwj@mail.iggcas.ac.cn)

Abstract: Short-lived giant mafic dyke swarms are keys to the interpretation of continental evolution and tectonics, reconstruction of continental palaeogeographical regimes, and petrogenesis of volcanism. The 1.78 Ga Taihang–Lvliang dyke swarm, one of the most significant and best-preserved Precambrian swarms in the central part of the North China craton (NCC), is reviewed and discussed. It is interpreted to have a radiating geometry that is compatible with the Xiong'er triple-junction rift, in which the Xiong'er volcanic province is proposed to be the extrusive counterpart of this swarm. It resulted in significant extension, uplift and magmatic accretion of the NCC, and it is comparable with the Phanerozoic large igneous provinces (LIPs) in areal extent (*c.* 0.3 Mkm²) and estimated volume (*c.* 0.3 Mkm³), short lifespan (<20 Ma), and intraplate setting. This North China LIP is unique in that it comprises large volumes of both mafic and intermediate components. It could have resulted from extensive mantle–crust interaction, probably driven by a large-scale mantle upwelling. A plume tectonic model is favoured by several lines of supporting evidence (i.e. massive volcanic flows correlated over large areas and a giant fanning dyke swarm with plume-affinitive chemistry). It could be responsible for massive sulphide (Pb–Zn) and gold (Au–Ag) ore deposits in the Xiong'er volcanic province. Dismembered remnants of this magmatism in other block(s), with potential candidates in South America, Australia and India, could identify other cratonic blocks that were formerly connected to the North China craton.

There are more than 100 giant mafic dyke swarms that extend for more than 300 km on planet Earth; thus far, the largest recognized is the Mackenzie swarm of the northern Canadian Shield, which extends for >2000 km (Ernst & Buchan 2001). Giant dyke swarms provide information on large-scale extension occurring in the continental lithosphere, and thus they are important in interpreting continental evolution and plate or plume tectonics (e.g. Ernst *et al.* 1995; Hanski *et al.* 2006). They serve as conduits transporting large volumes of magma from the mantle and thus contribute to growth of the continental crust. They could be the key to the petrogenesis of an overall magmatic event as they may preserve different and sometimes more primitive magma compositions, less affected by assimilation. They also provide a powerful tool in reconstructing ancient continental palaeogeography because of their large areal extent, well-defined and often short duration, palaeomagnetic record and inherent geometry (e.g. Bleeker & Ernst 2006). However, after their emplacement, dyke swarms may have been overprinted by later tectonothermal events resulting in deformation, metamorphism, displacement and dismemberment, and thus reconstruction is necessary prior to interpretation. Here, a case study on a 1.78 Ga giant dyke swarm in the North China craton is reviewed and discussed.

Geological background

The North China craton (NCC, also known as the Sino-Korean craton; Fig. 1) formed as a result of amalgamation of Archaean blocks either in the late Palaeoproterozoic (*c.* 1.85 Ga; e.g. Zhao, G.-C. *et al.* 2001, 2005; Wilde *et al.* 2002; Guo *et al.* 2005; Kröner *et al.* 2005), or alternatively in the latest Archaean (*c.* 2.5 Ga) followed by Palaeoproterozoic remobilization and re-cratonization (e.g. rifting, collision and/or uplift) (Li *et al.* 2000, 2002; Zhai *et al.* 2000; Kusky & Li 2003; Zhai & Liu 2003; Kusky *et al.* 2007a, b; Zhai & Peng 2007). After 1.8 Ga, the NCC stabilized, followed by episodes of rifting (1.8–1.6 Ga and *c.* 0.9 Ga; e.g. Zhu *et al.* 2005; Peng *et al.* 2008b) and platform deposition (1.6–1.4 Ga; e.g. Zhao, Z.-P. *et al.* 1993). Whether the NCC was involved in a palaeo-supercontinent (e.g. Nuna) or not, and where it may have been positioned in a global configuration have been widely discussed (e.g. Wilde *et al.* 2002; Zhao, G.-C. *et al.* 2002, 2004, 2010; Peng *et al.* 2005; Hou *et al.* 2008a). Many of these major events first shaping and then modifying the NCC were accompanied by mafic dyke swarms; that is, the 2.5 Ga Taipingzhai–Naoyumen dykes, the 2.15 Ga Hengling dykes and sills, the 1.97 Ga Xiwangshan dykes, the 1.96 Ga Xuwujia dykes, the 1.78 Ga Taihang–Lvliang dykes, the 1.76 Ga Beitai dykes, the

59
60
61
62
63
64
65
66
67
68
69
70
71
72
73
74
75
76
77
78
79
80
81
82
83
84
85
86
87
88
89
90
91
92
93
94
95
96
97
98
99
100
101
102
103
104
105
106
107
108
109
110
111
112
113
114
115
116

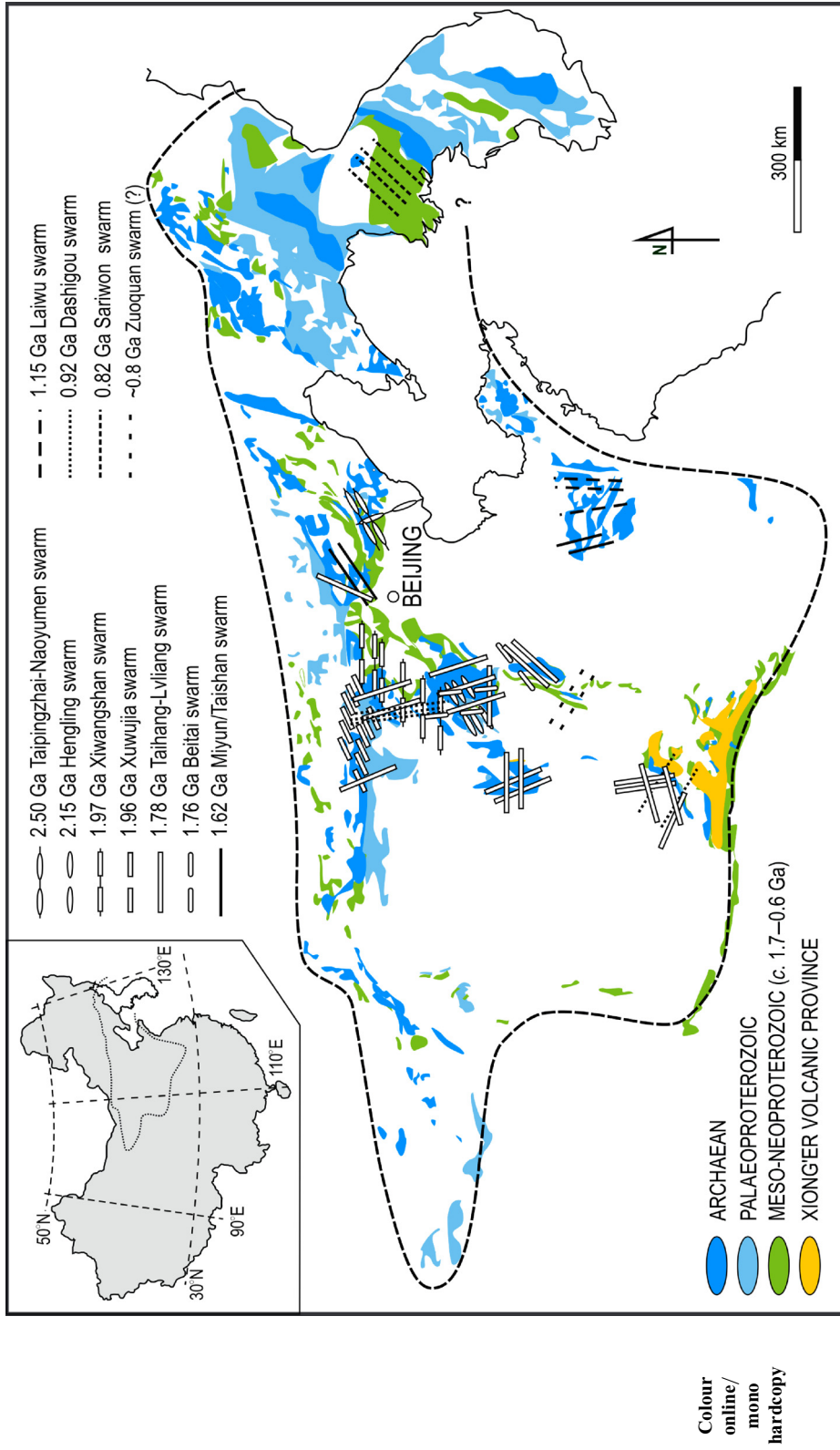


Fig. 1. Map showing the distribution of Precambrian mafic dykes and sills in the North China craton.

117 1.62 Ga Taishan–Miyun dykes, the 1.15 Ga Laiwu
 118 dykes, the 0.9 Ga Dashigou dykes, and the 0.9–
 119 0.8 Ga Sariwon and Zuoquan dykes (Fig. 1;
 120 Table 1). Each of these dyke swarms may provide
 121 important insights into the tectonothermal evolution
 122 of the Precambrian lithosphere of the NCC, and
 123 the possible palaeo-linkage(s) between the NCC
 124 and other craton(s). The 1.78 Ga Taihang–Lvliang
 125 swarm has a extent of *c.* 1000 km, and is the
 126 largest, most prominent and best-preserved Precam-
 127 brian swarm in the NCC (e.g. Qian & Chen 1987;
 128 Halls *et al.* 2000; Hou *et al.* 2000, 2005, 2008a;
 129 Peng *et al.* 2004, 2007; Wang *et al.* 2004, 2008).

132 Brief introduction to the 1.78 Ga 133 Taihang–Lvliang swarm

134 The Taihang–Lvliang dyke swarm (TLS) consists
 135 of NNW–SSE-trending (315° – 345°) dykes evenly
 136 distributed throughout the central NCC, as well as
 137 a few NE–SW- (20° – 40°) and east–west-trending
 138 (250° – 290°) dykes (Fig. 2). It was followed by a
 139 younger NNW–SSE-trending swarm with distinct
 140 compositions (the Beitai swarm, 1765 Ma; Wang
 141 *et al.* 2004; Peng *et al.* 2006; Fig. 3a). The NE–
 142 SW-trending dykes occur mainly in the South
 143 Taihang Mountains. The east–west dykes are res-
 144 tricted to the Lvliang, southern Taihang, Huoshan
 145 and Zhongtiao Mountains, and they locally cut or
 146 branch off the NNW–SSE dykes. The east–west
 147 dykes can be further distinguished into two groups,
 148 one trending between 250° and 270° (mainly in
 149 the Lvliang and Taihang Mts) and another group
 150 trending 270° – 290° (mainly in the Zhongtiao and
 151 Huoshan Mts) (Fig. 2).

152 The TLS dykes are up to 60 km long and up to
 153 100 m wide, with a typical width being *c.* 15 m.
 154 The dykes are vertical to subvertical and show
 155 sharp, chilled contacts with the country rocks. The
 156 systematic northward branching of the dykes indi-
 157 cates a magma flow direction from south to north
 158 (e.g. see Rickwood 1990). Mean ^{206}Pb – ^{207}Pb ages
 159 reported for the TLS dykes are 1769 ± 3 Ma (zircon
 160 thermal ionization mass spectrometry (TIMS), Halls
 161 *et al.* 2000), 1778 ± 3 Ma [zircon sensitive high-
 162 resolution ion microprobe (SHRIMP), Peng *et al.*
 163 2005], 1777 ± 3 Ma (zircon plus baddeleyite
 164 TIMS), and 1789 ± 28 Ma (baddeleyite TIMS)
 165 (Peng *et al.* 2006). An Ar–Ar age of about
 166 1780 Ma is also available (Wang *et al.* 2004). The
 167 TLS dykes are composed of gabbro and dolerite,
 168 with a mineralogy dominated by plagioclase and
 169 clinopyroxene. They are tholeiitic in composition,
 170 varying from basalt to andesite, with minor occur-
 171 rences of dacite and rhyolite. Peng *et al.* (2004,
 172 2007) chemically divided the TLS dykes into three
 173 groups, followed by a fourth group, now identified

as the Beitai swarm (Fig. 3a, b). It needs to be clari-
 fied that Wang *et al.* (2004) have also divided the
 dykes in South Taihang Mountains into three
 groups, on the basis of their chemistry, with their
 group 1 being compositionally similar to the NW
 group of the TLS dykes, their group 2 being
 similar to the Beitai swarm, and their group 3
 being distinct, possibly another swarm.

Geometrical reconstruction of the Taihang–Lvliang swarm

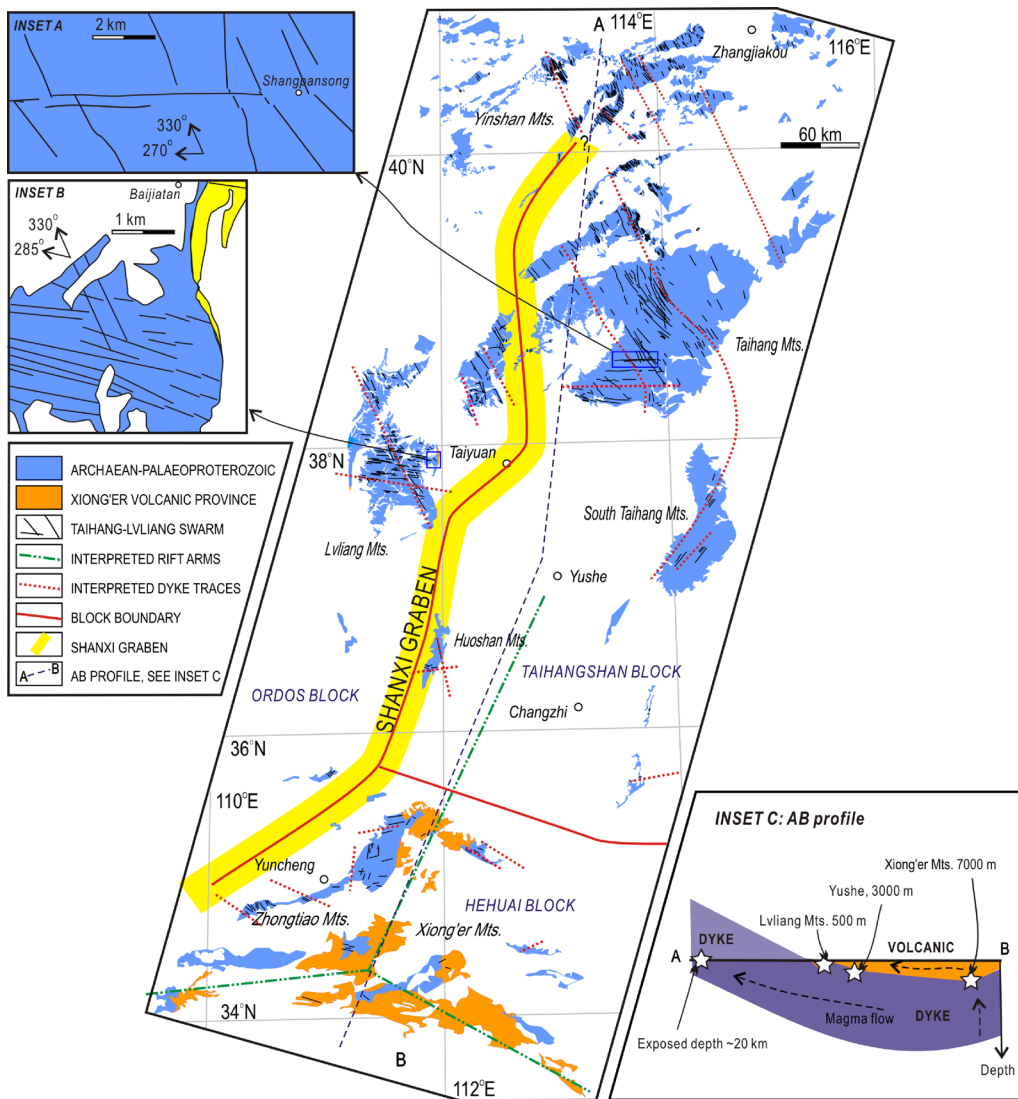
Because the orientations of the TLS dykes have
 been modified after their intrusion [for instance,
 the Taihangshan Block has recorded a *c.* 15° antic-
 lockwise rotation relative to the Ordos Block in
 the Mesozoic–Cenozoic (Fig. 2; e.g. Zhang *et al.* Q1
 2003; Huang *et al.* 2005)] the geometry of the
 dykes in these blocks needs to be reconstructed. In
 Figure 4a, the original orientations of dykes in the
 Taihang, South Taihang, Lvliang, Huoshan, Zhong-
 tiao and Xiong'er Mountains are shown together
 with reconstructed orientations suggested by palaeo-
 magnetic data (Zhang, Y.-Q. *et al.* 2003; Huang *et al.*
 2005). Figure 4b shows the presumed dyke tracks
 after restoration of the rotations. The dykes consti-
 tute a radiating pattern, which could fit the geo-
 metry of the Xiong'er triple-rift (the Xiong'er
 volcanic province); that is, the majority are consist-
 ent with the rift arm extending into the central NCC.
 The other two groups of east–west-trending dykes
 are parallel to other two arms of this rift. Qian &
 Chen (1987) and Hou *et al.* (2000) suggested that
 the east–west dykes are late intrusions that were
 emplaced in a different stress field. However, these
 east–west dykes are distribute only in the areas
 with lower exposure depths. Peng *et al.* (2008a)
 argued for two groups of dykes intruding into
 coeval fissures, either in a changing stress regime
 such as from plume-generated uplift to the onset of
 rifting and breakup, or in a single stress field with
 two groups of conjugate fissures at the uppermost
 crustal level, based on the observation of NNW–
 SSE- and east–west-trending dykes in a reticular
 fissure system. Also, the local crosscutting relation-
 ships (east–west dykes cutting NNW–SSE dykes)
 would have arisen during continuous intrusion
 and uplift.

Although it is difficult to reconstruct the possible
 coeval dykes in other parts of the NCC (e.g. the
 Taishan Mts, Hou *et al.* 2008b), this fanning geo-
 metry clearly indicates a stress field radiating from a
 magma centre as a result of uplift; that is, not
 simply compression or extension (e.g. a north–
 south compression; Hou *et al.* 2006). It is revealed
 that the dykes were uplifted and exhumed from
 crustal levels up to 20 km, mainly deep in the

Table 1. Precambrian mafic dyke swarms of the North China craton

Swarm	Present orientation(s)	Rocks	Series	Distribution	Scale (km)	Ages
Taipingzhai–Naoyumen Hengling	NW–SE and ENE–WSW Deformed	Gabbro Metagabbro (amphibolite schist)	Both tholeiitic and alkaline Tholeiitic	Eastern Hebei Wutai Mts.	> 100 c. 100	2504 ± 11 Ma, 2516 ± 26 Ma (zircon U–Pb), Li <i>et al.</i> (2010) 2147 ± 5 Ma (zircon U–Pb), Peng <i>et al.</i> (2005)
Xiawangshan	Deformed (ENE–WSW to east–west)	Metagabbro (high-pressure granulite)	Tholeiitic	Sanggan River	c. 200–300	1973 ± 4 Ma (zircon U–Pb), Peng <i>et al.</i> (2005)
Xuwujia	Deformed (ENE–WSW)	Metagabbro (high-temperature granulite)	Tholeiitic	Liangcheng–Tuguwu (Yinshan Mts.)	c. 200	1960 ± 4 Ma (zircon U–Pb), author's own unpublished data
Hengshan	Deformed (ENE–WSW)	Metagabbro (high-pressure granulite)	Tholeiitic	Hengshan Mts.	c. 100?	1914 ± 2 Ma, 1915 ± 4 Ma (zircon U–Pb), Kröner <i>et al.</i> (2006)
Taihang–Lvliang	NNW–SSE and east–west	Gabbro, dolerite	Tholeiitic	Central NCC and possibly other parts	c. 1000	1780–1770 Ma (present study)
Beitai	NNW–SSE to north–south	Gabbro	Tholeiitic	Hengshan–Taihang–South Taihang	> 200	1765 ± 1 Ma (Ar–Ar whole rock), Wang <i>et al.</i> (2004)
Miyun	NE–SW	Gabbro, dolerite	Tholeiitic	Miyun–Chengde	c. 100	1620 Ma (zircon U–Pb), author's own unpublished data
Taishan	NNW–SSE to NE–SW	Gabbro, dolerite	Tholeiitic	Taishan Mts.	c. 200?	1619 ± 16 Ma (baddeleyite Pb–Pb), Li, H.–M., <i>et al.</i> pers. comm.
Dashigou	NNW–SSE	Gabbro	Alkaline	Hengshan–Wutaihan Mts.	c. 300?	917 ± 7 Ma (baddeleyite Pb–Pb), author's unpublished data
Sariwon	ENE–WSW to east–west	Gabbro, dolerite	Tholeiitic	Pyongnam Basin, North Korea	c. 150	816 ± 34 Ma (zircon U–Pb); 884 ± 15 Ma (baddeleyite Pb–Pb), Peng <i>et al.</i> (2008b) and author's own unpublished data
Zuoquan	NW–SE	Gabbro, dolerite	Tholeiitic	Zuoquan and adjacent area	Unknown	Neoproterozoic, according to geological relationship

233
234
235
236
237
238
239
240
241
242
243
244
245
246
247
248
249
250
251
252
253
254
255
256
257
258
259
260
261
262
263
264
265
266
267
268
269
270
271
272
273
274
275
276
277
278
279
280
281
282
283
284
285
286
287
288
289
290



Colour
online/
mono
hardcopy

Fig. 2. Map showing the distribution of the Taihang–Lvliang swarm and Xiong'er volcanic province in the central NCC (after Peng *et al.* 2008a, with some younger dyke swarms, now dated and known to be unrelated, removed). Insets A and B show enlarged maps of local areas, and inset C is a profile of the study area based on the available geophysical (Wang 1995), geological (Peng *et al.* 2007) and palaeomagnetic data (Hou *et al.* 2000).

northern but shallow in the central study area according to the palaeomagnetic data (Hou *et al.* 2000) and a $P-T-t$ path (Peng *et al.* 2007). A north to south profile of the study area (Line AB in Fig. 2, inset c) can be constructed after incorporating seismic data in the south (e.g. Wang 1995). The increased uplift in the north of the study area could be partly responsible for the regional orientation changes of the dykes in the northern part of the central NCC (Fig. 4b); that is, the events resulting in this regional tilt could have distorted the orientations

of the dykes in the northern part. Figure 4c shows an idealized image of the possible geometry of the TLS dykes and Xiong'er rift system at 1.78 Ga.

The Xiong'er volcanic province: extrusive counterpart of the Taihang–Lvliang swarm?

The Xiong'er volcanic province (XVP) has been thought to have no genetic relationship with the

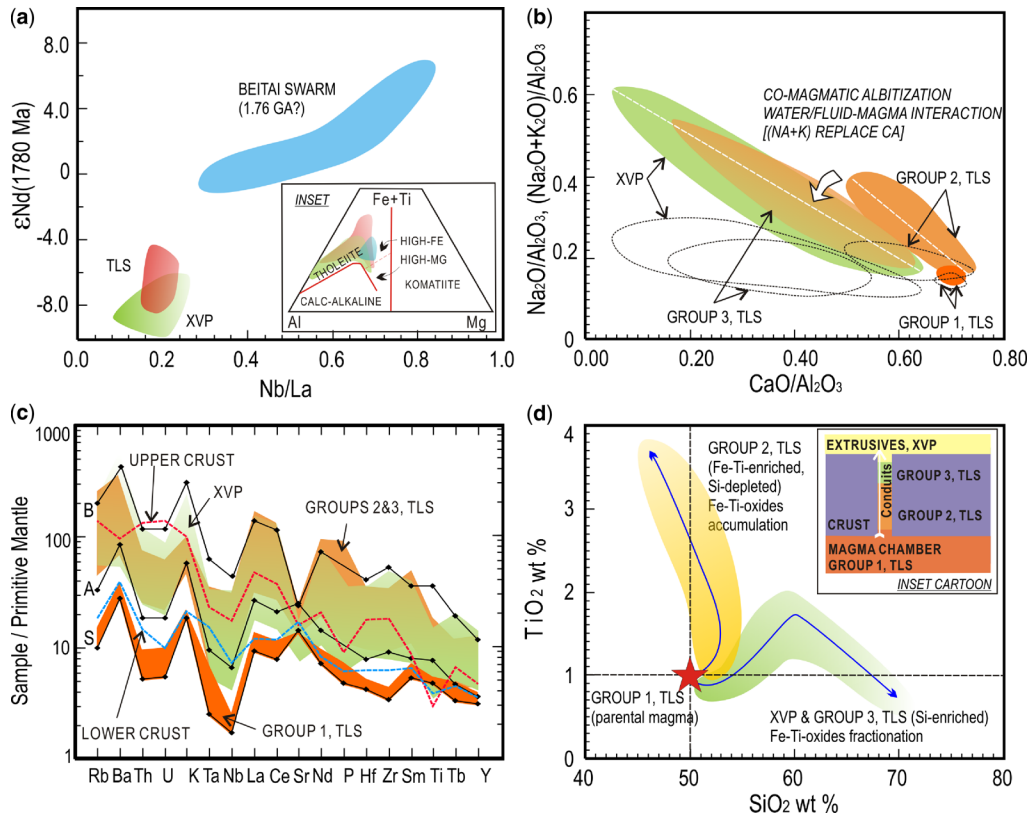


Fig. 3. (a) $\epsilon\text{Nd}(1780 \text{ Ma})$ v. Nb/La plot. Inset: $\text{Fe} + \text{Ti}$ v. Al v. Mg (mol) diagram (after Peng *et al.* 2007). (b) $\text{Na}_2\text{O}/\text{Al}_2\text{O}_3$ (open fields) and $(\text{Na}_2\text{O} + \text{K}_2\text{O})/\text{Al}_2\text{O}_3$ (coloured fields) v. $\text{CaO}/\text{Al}_2\text{O}_3$ plot. (c) Primitive mantle-normalized trace element spidergram of the Taihang–Lvliang dykes (TLS) and Xiong'er volcanic rocks (XVP): labelled curves refer to calculated liquid compositions after *in situ* crystallization (A) and fractional crystallization (B) from the starting composition (S) (after Peng *et al.* 2007). Primitive mantle-normalized values are after Sun & McDonough (1989). Data for the upper and lower crusts are after Rudnick & Gao (2001). (d) TiO_2 (wt%) v. SiO_2 (wt%) plot: the arrowed dashed lines show the differentiation trend, and the inset schematic illustration shows the relative differentiation depths of the TLS and XVP in the crust. Here Groups 1, 2 and 3 of TLS refer to the LT, NW and EW groups of Peng *et al.* (2007), respectively. Database is after Peng *et al.* (2008a).

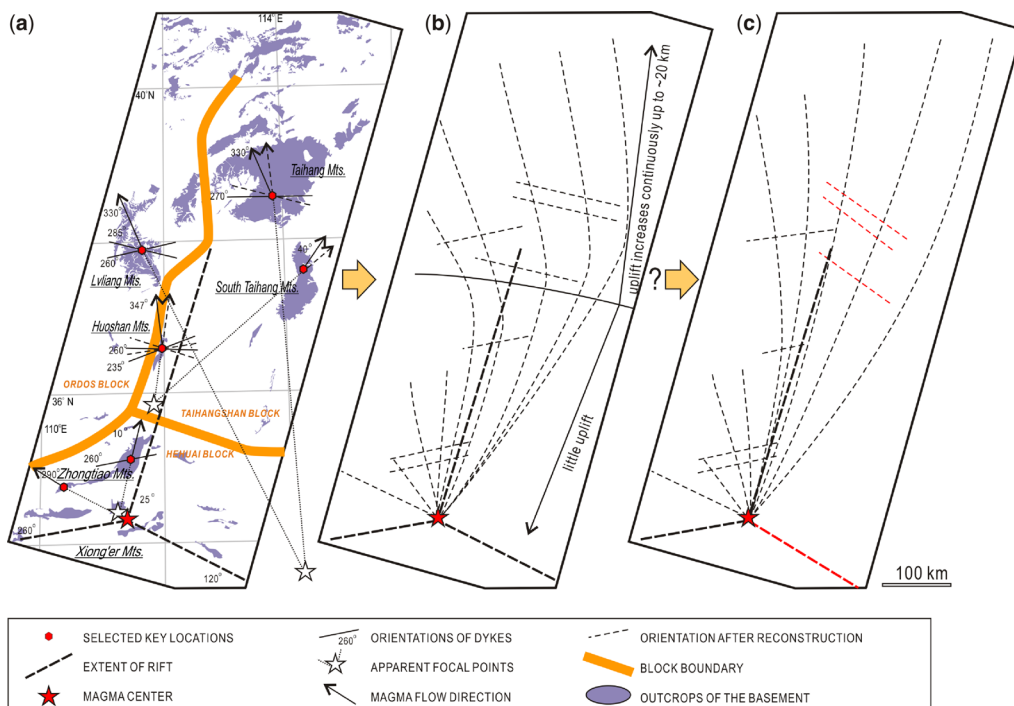
TLS as it is compositionally dominated by intermediate rather than mafic volcanic rocks (e.g. Pirajno & Chen 2005; He *et al.* 2008, 2009, and references therein). The XVP is located in the south of the NCC, and has three branches: two branches along the southern margin of the NCC and a third one extending northward into the interior of the NCC (Fig. 2). The XVP has a thickness of 3–7 km (Zhao, T.-P. *et al.* 2002) and is dominated by thick and continuous lava flows, with rare, thin, sedimentary and volcanoclastic interlayers. There are also minor pillow lavas. The XVP is composed of diabasic and porphyritic rock. It is chemically tholeiitic and varies from basalt to andesite, dacite and rhyolite, with andesitic compositions being dominant; thus the XVP does not resemble a

bimodal association. It consists of two volcanic cycles, both varying from mafic–intermediate to more silicic compositions; the age gap between the two cycles is not known. There are also some ultramafic bodies in the province, with associated Ni–Cu–PGE (platinum group elements) deposits, which are probably related to the XVP (Zhou *et al.* 2002). Ages of c. 1780–1770 Ma have been reported for the XVP (Zhao, T.-P. *et al.* 2004, 2005; Xu *et al.* 2007; He *et al.* 2009); however, some significantly younger ages have also been reported (He *et al.* 2009) but it remains unclear how these relate to the main XVP sequence.

The XVP is a host of important massive sulphide (Pb–Zn) and gold (Au–Ag) ore deposits in China, and there is evidence that the mineralization

Colour
online/
mono
hardcopy

349
350
351
352
353
354
355
356
357
358
359
360
361
362
363
364
365
366
367
368
369
370
371
372
373
374
375
376
377
378
379
380
381
382
383
384
385
386
387
388
389
390
391
392
393
394
395
396
397
398
399
400
401
402
403
404
405
406



Colour
online/
mono
hardcopy

Fig. 4. Geometry of the TLS and XVP: (a) orientations of the dykes and apparent magmatic focal points in the selected locations, and the extent of the rifts; (b) presumed geometry of the dykes after reconstruction in relation to the configuration of the rift; (c) idealized geometry of the dykes and the rifts based on model discussed in text.

could be associated with the volcanism. Some may have formed by (magmatic) fluid–rock interaction during the late stages of volcanism (e.g. Zhao, J.-N. *et al.* 2002; Hou *et al.* 2003; Ren *et al.* 2003; Zhang, H.-C. *et al.* 2003; Weng *et al.* 2006; Cao *et al.* 2008), especially in some fissures and vent complexes (Pei *et al.* 2007). This water (fluid)–rock interaction also caused albitization of feldspar, as well as alteration of the whole-rock chemistry, resulting in a spilite–keratophyre-type affinity in some of the XVP rocks (Peng *et al.* 2008a).

A cogenetic relationship between the XVP and TLS is favoured (i.e. the XVP is the extrusive counterpart of the TLS), because of the following observations: (1) the feeder dykes of the XVP have similar ages and compositions to the dykes of the TLS; (2) the geometries of the TLS (radiating fan) and XVP (triple-junction) are compatible with each other, and they share the same magmatic centre (Fig. 4b); (3) the exposure depths of the TLS and XVP are spatially correlated with the exhumation of the central NCC (Fig. 2, inset c); (4) they share similar petrographic characteristics, chemical variations (e.g. SiO₂ contents of the TLS and XVP

vary from 45 to 68 wt% and from 45 to 78 wt%, respectively), trace element patterns and isotopic compositions (Peng *et al.* 2008a). Further support for a cogenetic relationship comes from the observation that both the XVP rocks and a few of the TLS dykes have experienced co-magmatic albitization, resulted in the variations of certain major and trace elements (e.g. Na, Ca, K, Sr, Rb, etc., Peng *et al.* 2008a).

Thus the same parental magma, with varied degrees of differentiation and/or assimilation, can explain the petrogenesis of both the TLS and XVP. Figure 3c shows one possible model, which began with *in situ* crystallization, followed by assimilation and fractional crystallization, with an assemblage composed of plagioclase, clinopyroxene and olivine (Peng *et al.* 2008a). This model successfully interprets the variations of most trace elements and partly those of some major elements, excluding those altered by albitization. However, to explain the variations of some other elements (e.g. Fe and Ti) fractionation of Fe–Ti-oxides should be considered (Fig. 3d).

How then can we explain the apparent difference in dominant chemistry; that is, mafic (TLS) v.

intermediate (XVP)? The TLS is chemically divided into three groups: group 1 is minor and proposed as the parental magma composition of this magmatism; group 3 is intermediate-dominated and similar to the XVP; whereas group 2 forms most of the TLS and has very similar trace element patterns but partly distinguishable concentrations as compared with the XVP, especially for major elements (Table 2; Fig. 3c, d). The group 2 rocks show an Fe–Ti-enriched trend (Si-depleted), whereas the XVP rocks (and group 3) present a Si-enriched trend (Fig. 3d). It has been suggested that the liquid would have Fe–Ti enrichment when it differentiated in a closed system at a relatively low oxidation state, whereas it would be Si-enriched when it interacted with the oxidized and hydrated surroundings (Brooks *et al.* 1991). As the group 2 dykes are commonly exposed from greater depth than the group 3 dykes and the XVP (Peng *et al.* 2007), it is reasonable to propose that the corresponding liquid has evolved from being more mafic in the deeper crust to being more silicic at shallower depth (Fig. 3d). Also, as the iron-rich liquid is more dense and more difficult to erupt (e.g. Brooks *et al.* 1991), this more mafic liquid would crystallize along the margins of the dyke conduits, forming the mafic rocks (e.g. group 2). In the mean time, the remaining relatively more Si-rich liquid and also the fractionated liquid would interact and be incorporated with more oxidized and hydrated crust, fractionating more Fe–Ti-oxides, and produce more Si-rich liquid, forming the intermediate-dominated rocks (e.g. XVP and group 3) (Fig. 3d). Thus the differentiation of Fe–Ti-enriched liquid at great depth, as well as the continuous assimilation and fractionation (of plagioclase, clinopyroxene and olivine) during ascent, could be responsible for the average composition gap between the TLS and XVP (Table 2).

Another point is that some would argue that the XVP belongs to a calc-alkaline series, which makes it different from the tholeiitic TLS rocks (e.g. He *et al.* 2008, 2009, and references therein). However, this point of debate could be largely explained by the recognition of widespread albitization in the XVP and some of the TLS dykes (Han *et al.* 2006; Peng *et al.* 2008a; Fig. 3b). In this case, discrimination based on elements influenced by albitization (e.g. Na, K, Rb, Sr and Ca) should be avoided. In an Fe + Ti–Al–Mg diagram (Fig. 3a inset), both XVP and TLS samples plot in the tholeiitic field instead of the calc-alkaline field. It should be noted that most of the XVP samples, as well as many of the TLS samples, plot in the calc-alkaline field in a Th–Co diagram suitable for altered rocks (Zhao *et al.* 2009). However, this diagram is based on island arc rocks (Hastie *et al.* 2007), and has not yet been tested for

continental volcanic rocks, especially those with high Th content.

A large igneous province: lines of evidence and particularities

Large igneous provinces (LIPs) are considered to be massive crustal and intraplate emplacements of predominantly mafic extrusive and intrusive rocks that originated via processes other than ‘normal’ seafloor spreading (Coffin & Eldholm 1994, 2001). This definition has been extended to silicic provinces (Bryan *et al.* 2002; Sheth 2007; Bryan & Ernst 2008). Bryan & Ernst (2008) renewed this definition as those ‘magmatic provinces with areal extents $>0.1 \text{ Mkm}^2$, igneous volumes $>0.1 \text{ Mkm}^3$ and maximum lifespans of *c.* 50 Ma that have intraplate tectonic settings or geochemical affinities, and are characterized by igneous pulse(s) of short duration (*c.* 1–5 Ma), during which a large proportion ($>75\%$) of the total igneous volume is emplaced’. It should be noted that a minimal areal extent of 0.05 Mkm^2 (Sheth 2007) or 1 Mkm^2 (Courtillot & Renne 2003), and a lifespan of *c.* 1 Ma (e.g. Courtillot & Renne 2003) or $\geq 40 \text{ Ma}$ (e.g. Birkhold *et al.* 1999; Revillon *et al.* 2000) have been proposed.

Here, the area encompassed by Figure 2 is considered the estimated areal extent of the TLS, at *c.* 0.3 Mkm^2 . The XVP is continuous over a north–south extent of 500 km and an east–west extent of 360 km (Fig. 2; Wang 1995; Zhao *et al.* 2002; Xu *et al.* 2007); thus its areal extent can be calculated as $\frac{1}{2} \times 500 \text{ km} \times 360 \text{ km} = 0.09 \text{ Mkm}^2$, considering its triangular distribution. For the exposed areas, the areal extents are approximately 0.1 Mkm^2 and 0.02 Mkm^2 for the TLS and XVP, respectively (Fig. 2). The estimated magmatic volume of the TLS is calculated as: V (volume) = a (areal extent) $\times h$ (average height of the dykes) $\times \lambda$ (extension ratio). A height of 20 km is estimated based on an exposed depth (Peng *et al.* 2007) and the palaeomagnetic data (Hou *et al.* 2000). Although extension ratios ranging from 0.28 to 0.48% are available (Hou *et al.* 2006), three well-exposed profiles are further checked. These profiles, including the 25 km long Jvlebu–Zhangxiaocun (Datong), the 20 km long Hongqicun–Jiulongwan (Fengzhen) and the 50 km Doucun–Shengtangbu (Wutai) profiles, give extension ratios at 1.0%, 1.27% and 0.72%, respectively. The variation could be a result of uneven distribution and/or miscount. Here 1.0% is taken as the average extension ratio. Thus the estimated volume would be $V = 0.3$ ($a, \text{ Mkm}^2$) $\times 20$ ($h, \text{ km}$) $\times 1.0\%$ (λ) = 0.06 Mkm^3 , and the estimated exposed volume would be $V = 0.1$ (exposed area, Mkm^2) $\times 20$ ($h, \text{ km}$) $\times 1.0\%$ (λ) = 0.02 Mkm^3 . The volcanic volume of

Table 2. Average compositions of the Taihang–Lytang swarm (TLS) and the Xiong'er volcanic province (XVP), and the upper and lower crust

Contents (wt%)	Parental magma (Group 1, TLS)*	Group 2 (TLS) average*	Group 3 (TLS) TLS average*	TLS average*	XVP average*	TLS & XVP total average [†]	Lower crust [‡]	Upper crust [‡]
SiO ₂	50.09	50.29	56.66	51.55	57.69	56.27	53.40	66.60
TiO ₂	1.02	2.57	1.40	2.20	1.20	1.43	0.82	0.64
Al ₂ O ₃	14.85	13.00	14.23	13.41	14.11	13.95	16.90	15.40
Fe ₂ O ₃ (total iron)	13.31	15.47	10.18	14.22	9.39	10.50	8.57	5.04
MnO	0.19	0.20	0.14	0.19	0.14	0.15	0.10	0.10
MgO	6.99	4.02	3.62	4.20	3.49	3.65	7.24	2.48
CaO	10.31	7.45	5.69	7.35	4.58	5.22	9.59	3.59
Na ₂ O	2.27	2.65	2.45	2.58	2.92	2.84	2.65	3.27
K ₂ O	0.61	2.28	3.06	2.29	3.30	3.07	0.61	2.80
P ₂ O ₅	0.14	1.08	0.52	0.89	0.36	0.48	0.10	0.15
Total	99.76	99.01	97.95	98.86	97.17	97.56	99.98	100.07

*The TLS and XVP averages are based on a database from Peng *et al.* (2008a) (Groups 1, 2 and 3 correspond to the LT, NW and EW groups therein, respectively), and Group 1 (TLS) is proposed to represent the parental magma compositions.

[†]Total TLS and XVP average is calculated taking the estimated magma volumes as their weight.

[‡]The lower and upper crustal compositions are after Rudnick & Gao (2001).

465
466
467
468
469
470
471
472
473
474
475
476
477
478
479
480
481
482
483
484
485
486
487
488
489
490
491
492
493
494
495
496
497
498
499
500
501
502
503
504
505
506
507
508
509
510
511
512
513
514
515
516
517
518
519
520
521
522

the XVP is calculated using V (volume) = a (areal extent) $\times h$ (average thickness of the volcanic rocks). Assuming the original XVP extrusive extent as a triangular pyramid and taking the maximum exposed thickness of 7 km as an overall maximum, the volume would be $V = \frac{1}{3} \times 0.09$ (a , Mkm^2) $\times 7$ (h , km) $\approx 0.2 \text{ Mkm}^3$, and the exposed volume would be $V = 0.02$ (exposed area, Mkm^2) $\times 5$ (average thickness, km) = 0.1 Mkm^3 . Collectively, the TLS and XVP have a estimated total areal extent of $c. 0.3 \text{ Mkm}^2$, a volume of about 0.3 Mkm^3 , an exposed area of $c. 0.1 \text{ Mkm}^2$, and an exposed volume of $c. 0.1 \text{ Mkm}^3$. All these estimates could be doubled or even tripled if remnants in other parts of the NCC are confirmed, especially for the TLS.

The TLS and XVP postdate the regional granulite-facies metamorphism and amphibolite-facies retrograde metamorphism at 1790–1780 Ma (e.g. Wang *et al.* 1995; Zhang *et al.* 2006). They are followed by 1.75–1.73 Ga post-magmatic syenitic intrusions (Ren *et al.* 2000) and the 1.76 Ga Beitai swarm (Peng *et al.* 2008a). Thus the lifespan and duration of TLS and XVP magmatism is roughly bracketed to 1780–1760 Ma (i.e. about 20 Ma), even if the Beitai swarm is included. However, the duration of the major pulse is unknown. Undoubtedly, the magmatism has an intraplate tectonic affinity as it occurs largely within the NCC undergoing extension, and has within-plate compositional characteristics (see Bryan & Ernst 2008).

In summary, the 1.78 Ga magmatism including the TLS and XVP fits the LIP definition except for not knowing the duration of the major pulse (e.g. Bryan & Ernst 2008). There are several schemes for classification of LIPs; for instance, oceanic v. continental (Coffin & Eldholm 2001), mafic v. silicic (Bryan & Ernst 2008), and volcanic v. plutonic (Sheth 2007). It may be noted that most LIPs (both silicic and mafic dominated) are compositionally bimodal, and may also show a spectrum of compositions from basalt to high-silica rhyolite (e.g. Sheth 2007; Bryan & Ernst 2008). However, this North China LIP is characterized by more intermediate rocks than mafic rocks (with very few silicic components). The mafic portions are about 85% and 20% for the TLS and XVP, respectively (based on a database given by Peng *et al.* 2008a). The total mafic portion (p) could be $p_{\text{total}} = V_{\text{mafic}} / V_{\text{total}} = (p_{\text{TLS}} \times V_{\text{TLS}} + p_{\text{XVP}} \times V_{\text{XVP}}) / (V_{\text{TLS}} + V_{\text{XVP}}) \approx 35 \text{ vol.}\%$. In contrast, the intermediate portion could be $c. 65 \text{ vol.}\%$, as there are few other components. It should be mentioned that this mafic portion may be a minimum estimation, as the volume of TLS could be substantially underestimated.

Table 2 shows the average compositions of the TLS and XVP, their estimated total average, and their comparison with the average crust. Both the

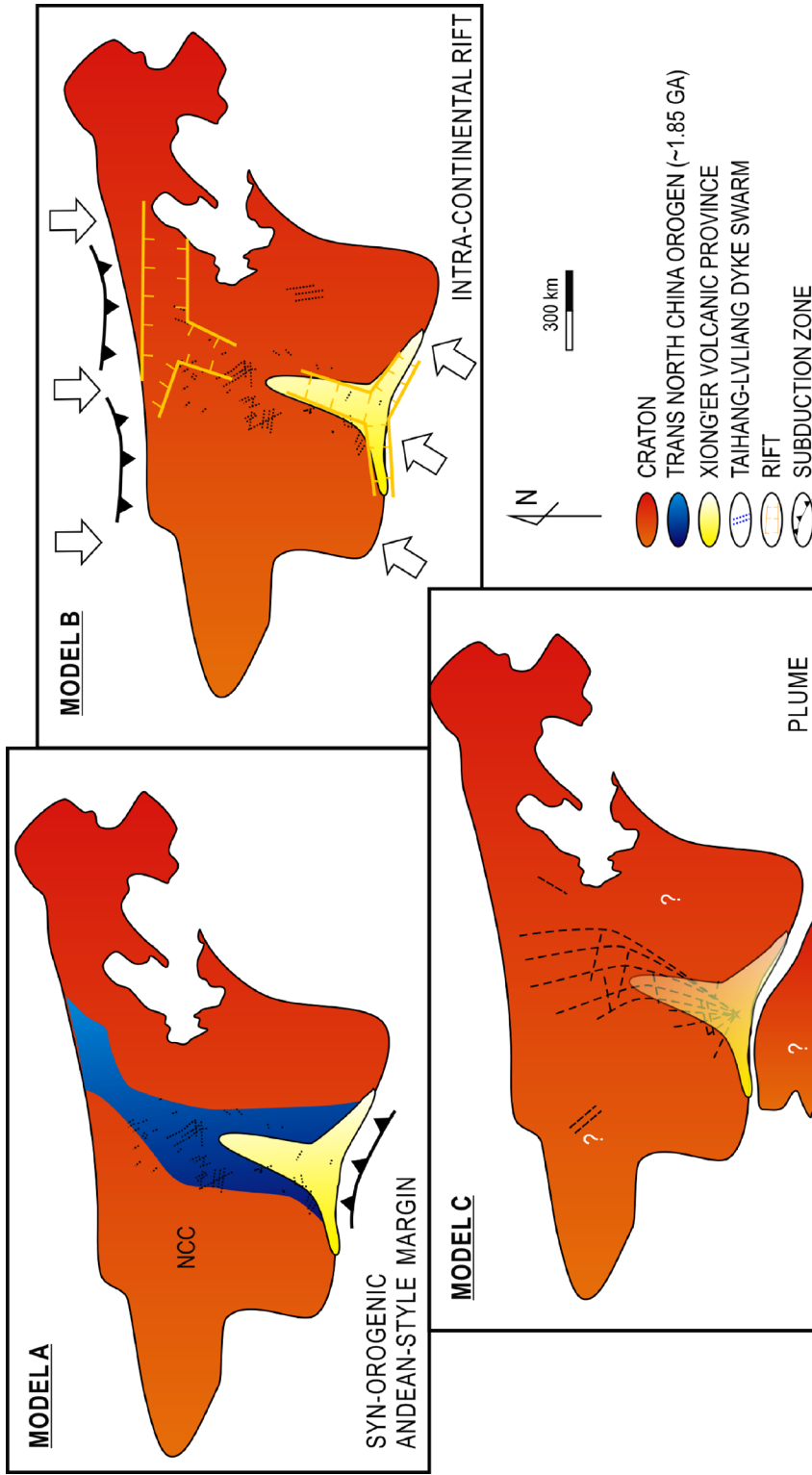
TLS and XVP averages, as well as their total average, show distinct characteristics from a potential melt from the lower or upper crust; for example, it would be difficult for the low Al_2O_3 content but high TiO_2 content to originate from the crust (Table 2, Fig. 3c). However, the total average of TLS and XVP is intermediate in composition (Table 2), which makes them in somewhat different from mantle-derived associations. In this case, incorporation of crustal melts in the parental magma (chamber) could be possible. However, it is still hard to evaluate this, as there is a possibility of underestimating the volume of TLS and thus the mafic weight in the total average. Nevertheless, some characteristics of the XVP, for example, slightly lower Nb and Ta but higher Th, U and Nd contents, as well as distinct higher Si concentration, compared with the TLS counterparts, could be partly inherited from the upper crust (e.g. Table 2; Fig. 3c). Thus it is reasonable to suggest that there are volumes of crustal melts incorporated into the magma during its ascent, especially for the late-stage differentiates (XVP).

Constraints on regional evolution and geodynamics

Reconstruction of the 1.78 Ga magmatism in the NCC (the TLS and XVP) increases its importance for the regional evolution and geodynamics. It indicates a broad rigid block undergoing significant extension and uplift at 1.78 Ga. It suggests that this rigid NCC block had basically ceased basement evolution from 1.78 Ga until the Mesozoic–Cenozoic, when the geometry of the TLS was distorted (Fig. 4). This implies a major magmatic accretion event at 1.78 Ga in the NCC, consistent with results from some $c. 1.8 \text{ Ga}$ mantle xenoliths (e.g. Gao *et al.* 2002).

Such reconstruction can also constrain the tectonic settings of the NCC at 1.78 Ga, as various alternatives have been proposed; that is, synorogenic (post-collisional uplift in the central NCC and Andean-style collision along its southern margin) (Fig. 5a; e.g. Zhao, G.-C. *et al.* 1998, 2010; Wang *et al.* 2004, 2008; He *et al.* 2008, 2009) or non-orogenic (Fig. 5b, c; e.g. Li *et al.* 2000; Zhai *et al.* 2000; Kusky & Li 2003; Hou *et al.* 2006, 2008a; Kusky *et al.* 2007b; Peng *et al.* 2004, 2008a). The synorogenic hypothesis is mainly based on the subduction-influenced geochemistry (e.g. depletion in high field strength elements) of both the TLS and XVP rocks, and Andean-style calc-alkaline volcanism. Nevertheless, the chemistry could alternatively be interpreted as affected by assimilation of the continental crust, or inherited from a fertilized mantle region. Also,

581
582
583
584
585
586
587
588
589
590
591
592
593
594
595
596
597
598
599
600
601
602
603
604
605
606
607
608
609
610
611
612
613
614
615
616
617
618
619
620
621
622
623
624
625
626
627
628
629
630
631
632
633
634
635
636
637
638



Colour
online/
mono
hardcopy

Fig. 5. Schematic illustrations showing tectonic models for the NCC at 1.78 Ga.

639 alteration and widespread albitization could explain
640 a resemblance of the XVP to an Andean-style
641 calc-alkaline association (in fact, it is tholeiitic,
642 see details given by Peng *et al.* 2008a). As the
643 TLS dykes have a radiating geometry (e.g. Fahrig
644 1987) and are very large scales (e.g. Ernst *et al.*
645 1995), they differ from synorogenic dykes; also,
646 as the XVP developed in a rift with triple-junction
647 geometry, with river–lake-facies sedimentary
648 interlayers, it is less compatible with a continental
649 margin environment.

650 However, instead of an intra-continental rift
651 model (Fig. 5b), a plume model (Fig. 5c) with
652 magma originating from a rifting centre is preferred
653 here because it meets four out of five criteria sug-
654 gested by Campbell (2001) to distinguish plume-
655 associated volcanism: (1) uplift prior to volcanism
656 (recorded by the 1.80–1.78 Ga regional P – T – t
657 paths and extensional deformation; e.g. Zhao,
658 G.-C. *et al.* 2005; Guo *et al.* 2005; Zhang *et al.*
659 2006, 2007); (2) a radiating dyke swarm geometry;
660 (3) massive volcanic flows correlated over a large
661 area (>0.09 Mkm²) and a long distance (>500 km);
662 (4) plume-associated chemistry (an enriched magma
663 source followed shortly by a depleted source with
664 OIB affinity; Peng *et al.* 2007). This plume possibly
665 could have responded to a massive mantle–crust
666 interaction to produce volumes of both mafic and
667 intermediate igneous rocks of the North China
668 LIP, as well as widespread polymetallic mineraliza-
669 tion in this area.

670 It should be addressed that this 1.78 Ga magma-
671 tism is centred in the southern most part of the NCC,
672 and thus it is reasonable to predict missing parts of
673 the TLS and/or XVP outside the NCC (Fig. 5c).
674 According to a database of Ernst & Buchan (2001),
675 roughly coeval (*c.* 1780 Ma) large mafic magmatic
676 events are reported in South America (e.g. Urugua-
677 yan dykes in Rio de Plata craton, Halls *et al.* 2001;
678 Avanavero dykes in Guyana shield, Norcross *et al.*
679 2000; Crepori gabbro–dolerite sills and dykes,
680 Santos *et al.* 2002), Australia (e.g. Harts Range vol-
681 canic rocks and sills and Eastern Creek volcanic
682 series, Sun 1997; Tewinga volcanic series, Page
683 1988; Mount Isa dykes, Parker *et al.* 1987; Hart
684 doleritic sills, Page & Hoatson 2000), and possibly
685 others (e.g. India: Dharwar dykes, Srivastava &
686 Singh 2004). All the above units are potential
687 candidates for the missing part(s) of the TLS and/
688 or XVP, providing clues to which blocks may
689 have been connected with the NCC.

691 Conclusions

694 Reconstruction and interpretation of ancient giant
695 mafic dyke swarms could be a potential way
696 to constrain ancient continental evolution and

geodynamics. As a case study, a radiating geometry
is reconstructed for the 1.78 Ga giant Taihang–
Lvliang swarm of the NCC. It can match the geom-
etry of the Xiong'er triple-junction rift, in which
the Xiong'er volcanic province is specified as the
extrusive counterpart of this swarm. This giant
radiating dyke swarm clearly indicates significant
extension, uplift, and magmatic accretion in the
NCC. Also, it could provide clues to potential lin-
kages between the NCC and other ancient block(s).
This dyke swarm, as well as the volcanic coun-
terpart, show affinities to Phanerozoic LIPs, and
could be the remnants of an ancient North
China LIP. However, this LIP is unique in that it
is characterized by large volumes of both mafic
(*c.* 35 vol.%) and intermediate (*c.* 65 vol.%) com-
ponents, which suggests extensive mantle–crust
interaction and notable differentiation in this
ancient plume setting.

I thank my many colleagues who have worked on this
subject, and have contributed much to it. I especially
acknowledge M. G. Zhai, J. H. Guo, T. P. Zhao, J. H. Li,
G. C. Zhao, G. T. Hou, S. W. Liu, Y. S. Wan, S. N. Lu,
H. M. Li, Y. H. He, Y. J. Wang, T. Kusky, H. Halls,
R. Ernst, W. Bleeker and S. Wilde. The paper has benefited
from criticism by two anonymous reviewers. I thank
B. Windley for his illuminating discussion and warm-
hearted encouragement. This study is financially supported
by China NSFC grant 40602024 and two previous grants
awarded to M. G. Zhai and T. P. Zhao.

References

- BIRKHOOD, A. B., NEAL, C. R., MAHONEY, J. J. &
DUNCAN, R. A. 1999. The Ontong Java plateau:
episode growth along the SE margin. *American
Geophysical Research*, **98**, 6607–6622.
- BLEEKER, W. & ERNST, R. 2006. Short-lived mantle
generated magmatic events and their dyke swarms:
the key unlocking Earth's paleogeographic record
back to 2.6 Ga. *In*: HANSKI, E., MERTANEN, S.,
RAMÖ, T. & VUOLLO, J. (eds) *Dyke Swarms – Time
Markers of Crustal Evolution*. Taylor & Francis,
London, 3–26.
- BROOKS, K. C., LARSEN, L. M. & NIELSEN, T. F. D. 1991.
Important of iron-rich tholeiitic magmas at divergent
plate margins: a reappraisal. *Geology*, **19**, 269–272.
- BRYAN, S. & ERNST, R. 2008. Revised definition of large
igneous provinces (LIPs). *Earth-Science Reviews*,
86, 175–202.
- BRYAN, S. E., RILEY, T. R., JERRAM, D. A., LEAT, P. T. &
STEPHENS, C. J. 2002. Silicic volcanism: an under-
valued component of large igneous provinces and vol-
canic rifted margins. *In*: MENZIES, M. A., KLEMPERER,
S. L., EBINGER, C. J. & BAKER, J. (eds) *Magmatic
Rifted Margins*. Geological Society of America,
Special Papers, **362**, 1–36.
- CAMPBELL, I. H. 2001. Identification of ancient
mantle plume. *In*: ERNST, R. E. & BUCHAN, K. L.
(eds) *Mantle Plumes: Their Identification through*

- 697 *Time*. Geological Society of America, Special Papers,
698 **352**, 5–21.
- 699 CAO, Y., LI, S.-R., SHEN, J.-F., YAO, M.-J., LI, Q.-K. &
700 MAO, F.-L. 2006. Fluid–rock interaction in ore-
701 forming process of Qianhe structure-controlled
702 alteration-type gold deposit in western Henan Pro-
703 vince. *Mineral Deposits*, **27**, 714–726 [in Chinese
704 with English abstract].
- 705 COFFIN, M. F. & ELDHOLM, O. 1994. Large igneous pro-
706 vinces: crustal structure, dimensions and external
707 consequences. *Reviews of Geophysics*, **32**, 1–36.
- 708 COFFIN, M. F. & ELDHOLM, O. 2001. Large Igneous Pro-
709 vinces: progenitors of some ophiolites? In: ERNST,
710 R. E. & BUCHAN, K. L. (eds) *Mantle Plumes: Their
711 Identification through Time*. Geological Society of
712 America, Special Papers, **352**, 59–70.
- 713 COURTILLOT, V. E. & RENNE, P. R. 2003. On the ages of
714 flood basalt events. *Comptes Rendus Geoscience*,
715 **335**, 113–140.
- 716 ERNST, R. E. & BUCHAN, K. L. 2001. Large mafic mag-
717 matic events through time and links to mantle plume
718 heads. In: ERNST, R. E. & BUCHAN, K. L. (eds)
719 *Mantle Plumes: Their Identification through Time*.
720 Geological Society of America, Special Papers, **352**,
721 483–575.
- 722 ERNST, R. E., HEAD, J. W., PARFITT, E., GROSFILS, E. &
723 WILSON, L. 1995. Giant radiating dyke swarms on
724 Earth and Venus. *Earth-Science Reviews*, **39**, 1–58.
- 725 FAHRIG, W. F. 1987. The tectonic settings of continental
726 mafic dyke swarms: failed arm and early passive
727 margin. In: HALLS, H. C. & FAHRIG, W. F. (eds)
728 *Mafic Dyke Swarms*. Geological Association of
729 Canada, Special Papers, **34**, 331–348.
- 730 GAO, S., RUDNICK, R. L., CARLSON, R. W., McDONOUGH,
731 W. F. & LIU, Y.-S. 2002. Re–Os evidence for
732 replacement of ancient mantle lithosphere beneath
733 the North China Craton. *Earth and Planetary Science
734 Letters*, **198**, 307–322.
- 735 GUO, J.-H., SUN, M., CHEN, F.-K. & ZHAI, M.-G. 2005.
736 Sm–Nd and SHRIMP U–Pb zircon geochronology
737 of high-pressure granulites in the Sanggan area,
738 North China Craton: timing of Palaeoproterozoic
739 continental collision. *Journal of Asian Earth Sciences*,
740 **24**, 629–642.
- 741 HALLS, H. C., LI, J.-H., DAVIS, D., HOU, G. T., ZHANG,
742 B.-X. & QIAN, X.-L. 2000. A precisely dated
743 Proterozoic paleomagnetic pole from the North China
744 craton, and its relevance to paleo-continental con-
745 struction. *Geophysical Journal International*, **143**,
746 185–203.
- 747 HALLS, H. C., CAMPAL, N., DAVIS, D. W. & BOSSI, J. 2001.
748 Magnetic studies and U–Pb geochronology of the
749 Uruguayan dyke swarm, Rio de la Plata craton,
750 Uruguay: paleomagnetic and economic implications.
751 *Journal of South American Earth Sciences*, **14**,
752 349–361.
- 753 HAN, Y.-G., ZHANG, S.-H., BAI, Z.-D. & DONG, J. 2006.
754 Albitization of the volcanic rocks of the Xiong'er
755 Group, Western Henan, and its implications. *Journal
756 of Mineralogy and Petrology*, **26**, 35–42 [in Chinese
757 with English abstract].
- 758 HANSKI, E., MERTANEN, S., RAMÖ, T. & VUOLLO, J.
759 (eds) 2006. *Dyke Swarms – Time Markers of Crustal
760 Evolution*. Taylor & Francis, London.
- HASTIE, A. R., KERR, A. C., PEARCE, J. A. & MITCHELL, S.
F. 2007. Classification of altered volcanic island arc
rocks using immobile trace elements: development
of the Th–Co discrimination Diagram. *Journal of
Petrology*, **48**, 2341–2357.
- HE, Y.-H., ZHAO, G.-C., SUN, M. & WILDE, S. 2008.
Geochemistry, isotope systematics and petrogenesis
of the volcanic rocks in the Zhongtiao Mountain: an
alternative interpretation for the evolution of the
southern margin of the North China Craton. *Lithos*,
102, 158–178.
- HE, Y.-H., ZHAO, G.-C., SUN, M. & XIA, X.-P. 2009.
SHRIMP and LA-ICP-MS zircon geochronology
of the Xiong'er volcanic rocks: implications for
the Paleo-Mesoproterozoic evolution of the southern
margin of the North China Craton. *Precambrian
Research*, **168**, 213–222.
- HOU, G.-T., LI, J.-H., QIAN, X.-L., ZHANG, B.-X. &
HALLS, H. C. 2000. The paleomagnetism and geologi-
cal significance of Mesoproterozoic dyke swarms in
the central North China craton. *Science in China (D)*,
44, 185–193.
- HOU, G.-T., LIU, Y.-L., LI, J.-H. & JIN, A.-W. 2005.
The SHRIMP U–Pb chronology of mafic dyke
swarms: a case study of Laiwu diabase dykes in
western Shandong. *Acta Petrologica et Mineralogica*,
24, 179–185.
- HOU, G.-T., WANG, C.-C., LI, J.-H. & QIAN, X.-L. 2006.
Late Palaeoproterozoic extension and a paleo-
stress field reconstruction of the North China Craton.
Tectonophysics, **422**, 89–98.
- HOU, G.-T., SANTOSH, M., QIAN, X.-L., LISTER, G. S. &
LI, J.-H. 2008a. Configuration of the Late Palaeo-
proterozoic supercontinent Columbia: insights from
radiating mafic dyke swarms. *Gondwana Research*,
14, 395–409.
- HOU, G.-T., LI, J.-H., YANG, M.-H., YAO, W.-H., WANG,
C.-C. & WANG, Y.-X. 2008b. Geochemical constraints
on the tectonic environment of the late Palaeoproter-
ozoic mafic dyke swarms in the North China Craton.
Gondwana Research, **13**, 103–116.
- HOU, W.-R., XIAO, R.-G., ZHANG, H.-C., GAO, L. & GAO,
D.-H. 2003. The genesis model of the gold–polymetal-
lic deposit from the volcanic rocks in the Xiong'er rift.
Gold Geology, **9**, 22–27 [in Chinese with English
abstract].
- HUANG, B.-C., SHI, R.-P., WANG, Y.-C. & ZHU, R.-X.
2005. Paleomagnetic investigation on Early–
Middle Triassic sediments of the North China block:
a new Early Triassic paleo-pole and its tectonic impli-
cations. *Geophysical Journal International*, **160**,
101–113.
- KRÖNER, A., WILDE, S. A., LI, J.-H. & WANG, K.-Y. 2005.
Age and evolution of a late Archaean to Palaeoproter-
ozoic upper to lower crustal section in the Wutaishan/
Hengshan/Fuping terrain of north China. *Journal of
Asian Earth Sciences*, **24**, 577–576.
- KRÖNER, A., WILDE, S. A. ET AL. 2006. Zircon geo-
chronology and metamorphic evolution of mafic
dykes in the Hengshan Complex of northern China:
Evidence for late Palaeoproterozoic extension
and subsequent high-pressure metamorphism in the
North China Craton. *Precambrian Research*, **146**,
45–67.

- 755 KUSKY, T. M. & LI, J.-H. 2003. Palaeoproterozoic tectonic
756 evolution of the North China craton. *Journal of Asian*
757 *Earth Sciences*, **22**, 383–397.
- 758 KUSKY, T., LI, J.-H. & SANTOSH, M. 2007a. The Palaeo-
759 proterozoic North Hebei Orogen: North China
760 craton's collisional suture with the Columbia super-
761 continent. *Gondwana Research*, **12**, 4–28.
- 762 KUSKY, T. M., WINDLEY, B. F. & ZHAI, M.-G. 2007b.
763 Tectonic evolution of the North China block: from
764 orogen to craton to orogen. In: ZHAI, M.-G.,
765 WINDLEY, B. F., KUSKY, T. M. & MENG, Q.-R. (eds)
766 *Mesozoic Sub-Continental Lithospheric Thinning*
767 *Under Eastern Asia*. Geological Society, London,
768 Special Publications, **208**, 1–34.
- 769 LI, J.-H., QIAN, X.-L., HUANG, X.-N. & LIU, S.-W. 2000.
770 The tectonic framework of the basement of north
771 China craton and its implication for the early Pre-
772 cambrian cratonization. *Acta Geologica Sinica*, **16**,
773 1–10.
- 774 LI, J.-H., KUSKY, T. M. & HUANG, X.-N. 2002. Neorarch-
775 ean podiform chromitites and mantle tectonites in
776 ophiolitic mélange, North China Craton: a record of
777 early oceanic mantle oceanic mantle processes. *GSA*
778 *Today*, **12**, 4–11.
- 779 LI, T.-S., ZHAI, M.-G., PENG, P., CHEN, L. & GUO, J.-H.
780 2010. Ca. 2.5 billion years old coeval ultramafic-
781 mafic and syenitic dykes in Eastern Hebei Region:
782 implications for cratonization of the North China
783 Craton. *Precambrian Research* (submitted).
- 784 NORCROSS, C., DAVIS, D. W., SPOONER, E. T. C. & RUST,
785 A. 2000. U–Pb and Pb–Pb age constraints on Palaeo-
786 proterozoic magmatism, deformation and gold
787 mineralization in the Omai area, Guyana Shield. *Pre-
788 cambrian Research*, **10**, 69–86.
- 789 PAGE, R. W. 1988. Geochronology of Early to Middle
790 Proterozoic fold belts in northern Australia: a review.
791 *Precambrian Research*, **40–41**, 1–19.
- 792 PAGE, R. W. & HOATSON, D. M. 2000. Geochronology
793 of mafic–ultramafic intrusions. In: HOATSON, D. M.
794 & BLAKE, D. H. (eds) *Geology and Economic Potential*
795 *of the Palaeoproterozoic Layered Mafic–Ultramafic*
796 *Layered Intrusions in the East Kimberley, Western*
797 *Australia*. Australian Geological Survey Organisation
798 Bulletin, **246**, 163–172.
- 799 PARKER, A. J., RICKWOOD, P. C. ET AL. 1987. Mafic dyke
800 swarms of Australia. In: HALLS, H. C. & FAHRIG, W.
801 F. (eds) *Mafic Dyke Swarms*. Geological Association
802 of Canada, Special Papers, **34**, 401–417.
- 803 PEI, Y.-H., YAN, H.-Q. & MA, Y.-F. 2007. The relationship
804 between paleo-volcanic apparatus and mineral
805 resources of Xiong'er Group along Songxian–Ruzhou
806 Zone in Henan Province. *Geology and Mineral*
807 *Resources of South China*, **1**, 51–58 [in Chinese with
808 English abstract].
- 809 PENG, P., ZHAI, M.-G., ZHANG, H.-F., ZHAO, T.-P. &
810 NI, Z.-Y. 2004. Geochemistry and geological signifi-
811 cance of the 1.8 Ga mafic dyke swarms in the North
812 China Craton: an example from the juncture of
813 Shanxi, Hebei and Inner Mongolia. *Acta Petrologica*
814 *Sinica*, **20**, 439–456 [in Chinese with English
815 abstract].
- 816 PENG, P., ZHAI, M.-G., ZHANG, H.-F. & GUO, J.-H. 2005.
817 Geochronological constraints on the Palaeoproterozoic
818 evolution of the North China Craton: SHRIMP zircon
819 ages of different types of mafic dikes. *International*
820 *Geology Review*, **47**, 492–508.
- 821 PENG, P., ZHAI, M.-G. & GUO, J.-H. 2006. 1.80–1.75 Ga
822 mafic dyke swarms in the central North China
823 craton: implications for a plume-related break-up
824 event. In: HANSKI, E., MERTANEN, S., RAMÖ, T. &
825 VUOLLO, J. (eds) *Dyke Swarms – Time Markers*
826 *of Crustal Evolution*. Taylor & Francis, London,
827 99–112.
- 828 PENG, P., ZHAI, M.-G., GUO, J.-H., KUSKY, T. & ZHAO,
829 T.-P. 2007. Nature of mantle source contributions
830 and crystal differentiation in the petrogenesis of the
831 1.78 Ga mafic dykes in the central North China
832 craton. *Gondwana Research*, **12**, 29–46.
- 833 PENG, P., ZHAI, M.-G., ERNST, R., GUO, J.-H., LIU, F. &
834 HU, B. 2008a. A 1.78 Ga Large Igneous Province
835 in the North China craton: The Xiong'er Volcanic
836 Province and the North China dyke swarm. *Lithos*,
837 **101**, 260–280.
- 838 PENG, P., ZHAI, M.-G., LI, Z., WU, F.-Y. & HOU, Q.-L.
839 2008b. Neoproterozoic (~820 Ma) mafic dyke swarms
840 in the North China craton: implication for a conjoint
841 to the Rodinia supercontinent? *Abstracts for the 13rd*
842 *Gondwana Conference, Dali, China*, 160–161. **Q10**
- 843 PIRAJNO, F. & CHEN, Y.-J. 2005. The Xiong'er Group:
844 a 1.76 Ga Large Igneous Province in East–Central
845 China? Available online at: [www.largeigneoupro-](http://www.largeigneouprovinces.org)
846 [vinces.org](http://www.largeigneouprovinces.org).
- 847 QIAN, X.-L. & CHEN, Y.-P. 1987. Late Precambrian mafic
848 dyke swarms of the North China craton. In: HALLS,
849 H. C. & FAHRIG, W. F. (eds) *Mafic Dyke Swarms*.
850 Geology Association of Canada, Special Papers, **34**,
851 385–391.
- 852 REN, F.-G., LI, S.-B., ZHAO, J.-N., DING, S.-X. & CHEN,
853 Z.-H. 2003. Te (Se) geochemical ore-hunting
854 information from the gold deposits in the volcanic
855 rocks of Xiong'er Group. *Geological Survey and*
856 *Research*, **26**, 45–51 [in Chinese with English
857 abstract].
- 858 REVILLON, S., ARNDT, N. T., CHAUVEL, C. & HALLOT, E.
859 2000. Geochemical study of ultramafic volcanic and
860 plutonic rocks from Gorgona Island, Colombia:
861 plumbing system of an oceanic plateau. *Journal of*
862 *Petrology*, **41**, 1127–1154.
- 863 RICKWOOD, P. C. 1990. The anatomy of a dyke and the
864 determination of propagation and magma flow direc-
865 tions. In: PARKER, A. J., RICKWOOD, P. C. & TUCKER,
866 D. H. (eds) *Mafic Dykes and Emplacement Mechan-*
867 *isms*. Balkema, Rotterdam, 81–100.
- 868 RUDNICK, R.-L. & GAO, S. 2001. Composition of the
869 continental crust. In: RUDNICK, R. L. (ed.) *Treatise*
870 *on Geochemistry, Volume 3, The Crust*. Elsevier,
871 Amsterdam, 1–64.
- 872 SANTOS, J. O. S., HARTMANN, L. A., MCNAUGHTON, N. J.
873 & FLETCHER, I. R. 2002. Timing of mafic magmatism
874 in the Tapajos Province (Brazil) and implications for
875 the evolution of the Amazon craton: evidence from
876 baddeleyite and zircon U–Pb SHRIMP geochronol-
877 ogy. *Journal of South American Earth Sciences*, **15**,
878 409–429.
- 879 SHEATHE, H. C. 2007. 'Large Igneous Provinces (LIPs)':
880 definition, recommended terminology, and a hier-
881 archical classification. *Earth-Science Reviews*, **85**,
882 117–124.

- 813 SRIVASTAVA, K. R. & SINGH, R. K. 2004. Trace element
814 geochemistry and genesis of Precambrian sub-alkaline
815 mafic dikes from the central Indian craton: evidence
816 for mantle metasomatism. *Journal of Asian Earth
817 Sciences*, **23**, 373–389.
- 818 SUN, S.-S. 1997. Chemical and isotopic features of
819 Palaeoproterozoic mafic igneous rocks of Australia:
820 implications for tectonic processes. In: SAUNDERS,
821 R. W. R. & DRUMMOND, B. J. (eds) *Palaeoproterozoic
822 Tectonics and Metallogenesis: Comparative Analysis
823 of Parts of the Australian and Fennoscandian
824 Shields*. Australian Geological Survey Organization
825 Record, **44**, 119–122.
- 826 SUN, S.-S. & McDONOUGH, W. F. 1989. Chemical and
827 isotopic systematics of oceanic basalts: implications
828 for mantle composition and processes. In: SAUNDERS,
829 A. D. & NORRY, M. J. (eds) *Magmatism in the Ocean
830 Basins*. Geological Society, London, Special Publi-
831 cations, **42**, 313–354.
- 832 WANG, S.-S., SANG, H.-Q., QIU, J., CHEN, M.-E. & LI,
833 M.-R. 1995. The metamorphic age of pre-Changcheng
834 system in Beijing–Tianjin area and a discussion about
835 the lower limit age of Changcheng system. *Scientia
836 Geologica Sinica*, **30**, 348–354.
- 837 WANG, T.-H. 1995. Evolutionary characteristics of
838 geological structure and oil–gas accumulation in
839 Shanxi–Shaanxi area. *Journal of Geology and
840 Mineral Resource of North China*, **10**, 283–398 [in
841 Chinese with English abstract].
- 842 WANG, Y.-J., FAN, W.-M., ZHANG, Y.-H., GUO, F.,
843 ZHANG, H.-F. & PENG, T.-P. 2004. Geochemical,
844 $^{40}\text{Ar}/^{39}\text{Ar}$ geochronological and Sr–Nd isotopic
845 constraints on the origin of Palaeoproterozoic mafic
846 dikes from the southern Taihang Mountains and
847 implications for the ca. 1800 Ma event of the North
848 China Craton. *Precambrian Research*, **135**, 55–77.
- 849 WANG, Y.-J., ZHAO, G.-C., CAWOOD, P. A., FAN, W.-M.,
850 PENG, T.-P. & SUN, L.-H. 2008. Geochemistry of
851 Palaeoproterozoic (~1770 Ma) mafic dikes from the
852 Trans-North China Orogen and tectonic implications.
853 *Journal of Asian Earth Sciences*, **33**, 61–77.
- 854 WENG, J.-C., LI, Z.-M., YANG, Z.-Q. & LI, W.-Z. 2006.
855 Hydrothermally modified Pb–Zn deposit: a new
856 deposit type in volcanic rocks of the Xiong'er Group,
857 Henan, China. *Geological Bulletin of China*, **25**,
858 502–505 [in Chinese with English abstract].
- 859 WILDE, S. A., ZHAO, G.-C. & SUN, M. 2002. Develop-
860 ment of the North China craton during the Late
861 Archaean and its final amalgamation at 1.8 Ga: some
862 speculation on its position within a global Palaeo-
863 proterozoic Supercontinent. *Gondwana Research*,
864 **5**, 85–94.
- 865 XU, Y.-G., CHUNG, S.-L., JAHN, B.-M. & WU, G.-Y. 2001.
866 Petrologic and geochemical constraints on the petro-
867 genesis of Permian–Triassic Emeishan flood basalts in
868 southwestern China. *Lithos*, **58**, 145–168.
- 869 ZHAI, M.-G. & LIU, W.-J. 2003. Palaeoproterozoic
870 tectonic history of the North China craton: a review.
871 *Precambrian Research*, **122**, 183–199.
- 872 ZHAI, M.-G. & PENG, P. 2007. Palaeoproterozoic events
873 in the North China Craton. *Acta Petrologica Sinica*,
874 **23**, 2665–2682.
- 875 ZHAI, M.-G., BIAN, A.-G. & ZHAO, T.-P. 2000. Amalga-
876 mation of the supercontinental of the North China
877 craton and its break up during late–middle Protero-
878 zoic. *Science in China (Series D)*, **43**, 219–232.
- 879 ZHANG, H.-C., XIAO, R.-G., AN, G.-Y., ZHANG, L., HOU,
880 W.-R. & FEI, H.-C. 2003. Hydrothermal mine-
881 ralization of Au(Ag)-polymetallic ore deposit in the
882 volcanic rock series of the Xiong'er Group.
883 *Geology in China*, **34**, 400–405 [in Chinese with
884 English abstract].
- 885 ZHANG, H.-F., ZHAI, M.-G. & PENG, P. 2006. Zircon
886 SHRIMP U–Pb age of the Palaeoproterozoic high-
887 pressure granulites from the Sanggan area, the North
888 China craton and its geologic implications. *Earth
889 Science Frontiers*, **13**, 190–199 [in Chinese with
890 English abstract].
- 891 ZHANG, J., ZHAO, G.-C. ET AL. 2007. Structural, geochro-
892 nological and aeromagnetic studies of the Hengshan–
893 Wutai–Fuping mountain belt: implications for the
894 tectonic evolution of the trans-North China Orogen.
895 *Abstracts of National Conference on Petrology and
896 Geodynamics 2007*, 200–201. **Q11**
- 897 ZHANG, Y.-Q., MA, Y.-S., YANG, N., SHI, W. & DONG,
898 S.-W. 2003. Cenozoic extensional stress evolution in
899 North China. *Journal of Geodynamics*, **36**, 591–613.
- 900 ZHAO, G.-C., WILDE, S. A., CAWOOD, P. A. & SUN, M.
2001. Archaean blocks and their boundaries in the
North China craton: lithological, geochemical, struc-
tural and P–T path constraints and tectonic evolution.
Precambrian Research, **107**, 45–73.
- ZHAO, G. C., SUN, M. & WILDE, S. A. 2002. Review
of global 2.1–1.8 Ga orogens: implications for a
Pre-Rodinia supercontinent. *Earth-Science Reviews*,
59, 125–162.
- ZHAO, G. C., SUN, M., WILDE, S. A. & LI, S. Z. 2004.
A Paleo-Mesoproterozoic supercontinent: assembly,
growth and breakup. *Earth-Science Reviews*, **67**,
91–123.
- ZHAO, G.-C., SUN, M., WILDE, S. A. & LI, S.-Z. 2005.
Late Archaean to Palaeoproterozoic evolution of
the North China craton: key issues revisited. *Precam-
brian Research*, **136**, 177–202.
- ZHAO, G.-C., HE, Y.-H. & SUN, M. 2010. The Xiong'er
volcanic belt at the southern margin of the North
China Craton: petrographic and geochemical evidence
for its outboard position in the Paleo-Mesoproterozoic
Columbia Supercontinent. *Gondwana Research* (in
press). **Q12**
- ZHAO, J.-N., REN, F.-G. & LI, S.-B. 2002. Characters
and significance of amygdaloidal fabric copper ore
in Dasheping copper mine, Ruyang, Henan Province.
Progress in Precambrian Research, **25**, 97–104
[in Chinese with English abstract].
- ZHAO, T.-P., ZHOU, M.-F., ZHAI, M.-G. & XIA, B. 2002.
Palaeoproterozoic rift-related volcanism of the
Xiong'er group, North China craton: implications for
the breakup of Columbia. *International Geology
Review*, **44**, 336–351.
- ZHAO, T.-P., ZHAI, M.-G., XIA, B., LI, H.-M., ZHANG,
Y.-X. & WANG, Y.-S. 2004. Zircon U–Pb SHRIMP
dating for the volcanic rocks of the Xiong'er Group:
constraints on the initial formation age of the cover
of the North China craton. *Chinese Science Bulletin*,
49, 2495–2502.
- ZHAO, T.-P., WANG, J.-P. & ZHANG, Z.-H. (eds)
2005. *Proterozoic Geology of Mt. Wangwushan and*

- 871 *Adjacent Areas, China*. China Dadi Publishing House,
872 Beijing.
- 873 **Q13** ZHAO, Z.-P. ET AL. 1993. *Precambrian Crustal Evolution*
874 *of the Sino-Korean Para-platform*. Science Press,
875 Beijing.
- 876 ZHOU, M.-F., YANG, Z.-X., SONG, X.-Y., KEAYS, R. R. &
877 LESHNER, C. M. 2002. Magmatic Ni–Cu–(PGE)
878 sulphide deposits in China. *CIM Special Volume*, **54**,
879 619–636.
- 880 ZHU, S.-X., HUANG, X.-G. & SUN, S.-F. 2005. New pro-
881 gress in the research of the Mesoproterozoic Chang-
882 cheng system (1800–1400 Ma) in the Yanshan range,
883 North China. *Journal of Stratigraphy*, **19**, 437–449
884 [in Chinese with English abstract].
- 885
- 886
- 887
- 888
- 889
- 890
- 891
- 892
- 893
- 894
- 895
- 896
- 897
- 898
- 899
- 900
- 901
- 902
- 903
- 904
- 905
- 906
- 907
- 908
- 909
- 910
- 911
- 912
- 913
- 914
- 915
- 916
- 917
- 918
- 919
- 920
- 921
- 922
- 923
- 924
- 925
- 926
- 927
- 928